AN INVESTIGATION OF PYCLEN METAL CHELATOR RELEASE ON THE AGGREGATION OF AMYLOID-BETA

by

Caroline Crittell

Submitted in partial fulfillment of the
requirements for Departmental Honors in
the Department of Chemistry & Biochemistry
Texas Christian University
Fort Worth, Texas

May 6, 2024

AN INVESTIGATION OF PYCLEN METAL CHELATOR RELEASE ON THE AGGREGATION OF AMYLOID-BETA

Project Approved:

Supervising Professor: Jeffery Coffer, Ph.D.

Department of Chemistry & Biochemistry

Kayla Green, Ph.D.

Department of Chemistry & Biochemistry

Giri Akkaraju, Ph.D.

Department of Biology

ABSTRACT

Alzheimer's Disease (AD) affects over 6.5 million Americans over the age of 65. Previous research links AD with Amyloid-Beta-40 (Aβ) aggregation in the brain, which creates neurotoxic plaques, associated with AD. A potential mechanism in the treatment of AD is using therapeutics that will prevent the formation of these plaques, which is possible with Metal ion chelation therapy.

Metal ion chelation therapy ideally stops metal ions from aiding in the aggregation of Aβ. However, to deliver metal chelating agents to the brain, a drug-delivery mechanism is required that will be able to deliver this potential therapeutic across the Blood-Brain Barrier. Mesoporous silica is a potential drug delivery material due to its small particle size, high loading capacity, surface tunability, and biocompatibility. Along with these characteristics, mesoporous silica can create a sustained release profile of a given therapeutic, allowing for a slow and steady release profile, reducing the risks of medication side effects.

This project seeks to establish the optimal loading capacities of a class of potential metal ion chelate therapeutic molecules known as pyclens into mesoporous silica, each with different pyridyl moieties and chemical functionalities along the rim of the molecule. Loading capacity measurements for these pyclen derivatives reveal loading percentages in the 10-25% range, varying by pyclen identity. Additionally, release studies monitored diffusion over time to find which pyclen molecule achieved "sustained" release. All loaded pyclen species were able to show sustained release after 20 minutes, both in the presence and absence of copper metal ions (Cu^{2+}). Turbidity assays with Aβ present showed that all pyclen species decreased protein aggregation in the presence of Cu^{2+} metal ions, relative to non-pyclen controls, showing that all pyclen species were able to successfully prevent the aggregation of Aβ in the presence of Cu^{2+} metal ions.

ACKNOWLEDGEMENTS

This work would not have been possible without the guidance and support of many in the TCU Chemistry and Biochemistry Department.

First, I would like to thank Dr. Coffer for serving as my research advisor on this project. Over the years as a mentor, he has offered me encouragement, patience, advice, and optimism throughout the completion of this work. Thank you for helping me grow so much as a researcher and person over my years at TCU. I am extremely grateful to have him as a research advisor and mentor.

I also want to thank all of my lab mates in the Coffer Research group; Will, Maeggyn, Leo, George, Sarafina, Nhu, and Dylan, all of whom made my lab experience so enjoyable. I am grateful for all of the support and guidance offered to me by them, and for making our lab such a wonderful environment to work in. I also want to thank Youanna Ibrahim, a former student in the Coffer lab who began this project, who I am grateful for offering me advice and guidance in this project. I am also grateful for Dr. Kayla Green and Dr. Giri Akkaraju for sharing their knowledge and advice with me to help shape this project.

Finally, I want to thank my family and friends, all of whom were there for me throughout this project, offering encouragement and their support. Thank you for celebrating with me in the highs and being with me in the lows of this project and throughout my time in college. Everything that I achieve is possible because of the love and support they offer me.

Table of Contents

List of Figures

1. Introduction

It is estimated by the Alzheimer's Association that as of 2023, 6.7 million Americans are living with Alzheimer's Disease (AD) today.[1] AD is a form of dementia that causes a gradual shrinking of the brain and brain cell death, resulting in memory loss, as well as declines in social skills and cognitive abilities. While certain risk factors for the disease are understood, the exact cause of AD is unknown.[2]

Not only is AD a huge burden on individuals suffering from this disease and their caretakers, but it is also a financial burden on our healthcare system. It was estimated by the Alzheimer's Association that in 2023, $345 billion was spent on AD care.[1] Finding out more about AD and its pathology may help guide research towards more impactful treatments, helping to improve the lives of millions of Americans and saving our healthcare system billions of dollars.

While a cure has not been found, research about the pathology of AD has been conducted in hopes of understanding what physical structures are associated with AD. Most literature sources point to Amyloid-β (Aβ) as a major component of AD pathology.[3,4] Amyloid-Precursor Protein (APP) can be cleaved at different amino acid residues, and one of these cleavages can lead to the production of Aβ. When Aβ is first produced, it has lower amounts of beta-sheet motifs present. As it forms beta-sheets in its structure, it oligomerizes and interacts with other Aβ proteins with higher concentrations of beta-sheets. When this oligomer reaches a certain size, it will become insoluble Aβ plaques, which are toxic. Aggregated, Aβ plaque structures are a hallmark of AD pathology.[5]

The Amyloid Hypothesis and understanding the role Aβ plays in AD has led to lots of research involving Aβ. Specifically, what causes Aβ to misfold and what techniques and interventions could possibly prevent the misfolding of Aβ.[6] It is well established that metal ions exacerbate Aβ plaque

formation.[7] Correct metal ion concentration in the brain and throughout the body is important for many enzymatic functions and bodily functions. However, incorrect levels of metal ions can lead to dysfunction and disease. In the case of AD, higher levels of copper (Cu^{2+}) metal ions are associated with AD.[8] This is also observed in mice studies, where it was observed that Cu^{2+} metal ion exposure led to increased levels of both APP and Aβ in the brain.[9]

With the knowledge of the role that metal ions potentially play in the development of AD, metal chelation therapy has been considered as a possible treatment for AD to prevent Aβ aggregation.[10] Metal chelation therapy uses metal ion scavenger ligands to trap and sequester metal ions. In the case of Aβ, this could inhibit metal ions from accelerating the Aβ aggregation process. Many metal chelators are ligands containing Lewis Base moieties at selected positions in carbon rings present in the ligand, in some cases nitrogen or sulfur.

The Green Chemistry group at Texas Christian University has an extensive library of ligands that are ideally designed for this purpose. Not only do these ligands contain metal chelating capabilities from their cyclen ring structure, but they also possess antioxidant properties with the incorporation of a pyridine ring.[11,12] Figure 1 shows the available ligands that were used in this study. These ligands differ in their antioxidant abilities based on the number of pyridine rings they contain, and their electrical and chemical properties are a function of the functional groups that are substituted in their para-pyridine ring positions. Substitutions are present in the para-position of the pyridine rings due to their accessibility during the synthesis of these pyclen groups. L1 through L4 are the labels used to describe each ligand used in this research.

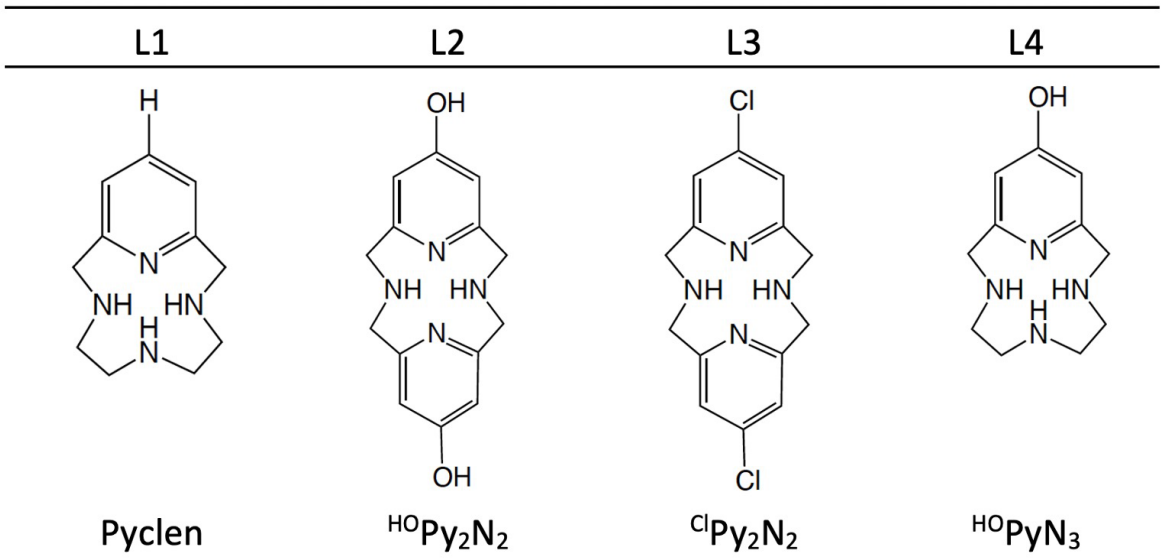

Figure 1. Selected metal chelators of the pyclen class, courtesy of Dr. Kayla Green and the Green Group, TCU.

Our hypothesis is that in this therapeutic method, sequestering metal ions away from Aβ proteins will prevent plaque formation, slowing or preventing the formation of pathological structures associated with AD. However, there are still many challenges to overcome to make metal chelation therapy a possible treatment. One of the biggest challenges is getting these ligands across the Blood-Brain Barrier (BBB).[10] The BBB is the physical barrier that separates the blood in the central nervous system (CNS) from the blood in the rest of our body. This serves the important role of protecting the CNS from toxins and infection, but it makes it difficult to deliver potential therapeutics to the CNS.[13] Despite these obstacles, researchers are still trying to develop delivery systems for therapeutics to successfully pass the BBB to treat neurodegenerative diseases, including AD.

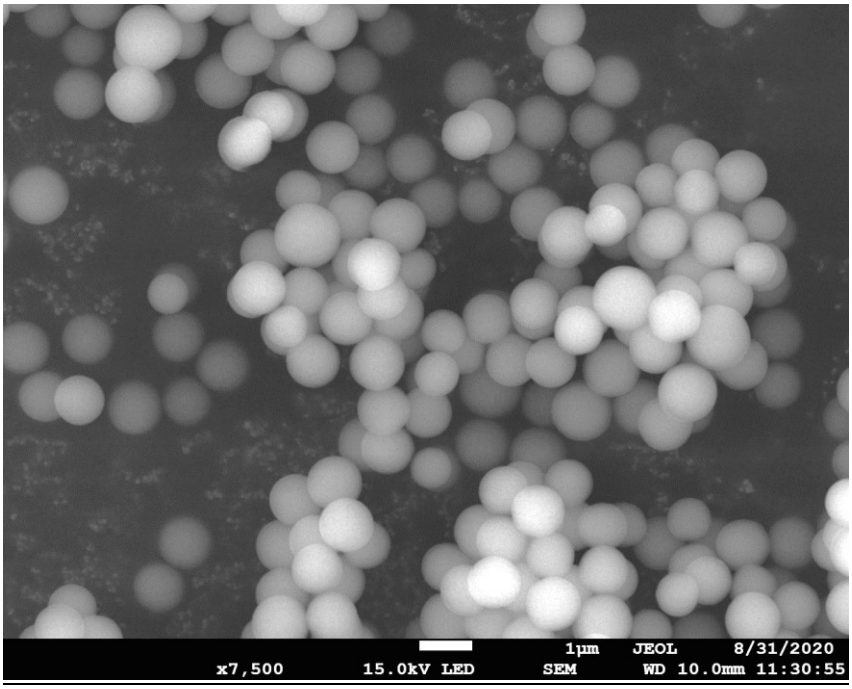

Figure 2. SEM image of 1μM mesoporous silica, 2nm pore size, Courtesy of William Burnett, TCU Department of Chemistry & Biochemistry.

One material currently being explored for its drug delivery capabilities is mesoporous silica ($pSiO_2$). $pSiO_2$ is ideal for drug delivery due to its high surface area and loading capacity, biocompatibility, and its tunability in relation to its pore sizes. $pSiO_2$ is also currently being investigated for a variety of medicinal applications outside of drug delivery, including cancer therapy, bioimaging, and biosensing.[14,15]

Previous researchers have used silica as their Alzheimer therapeutic delivery device. This was seen in the work of Wang et al.[16] Using SiO_2 as their delivery material, ligands used in their studies were covalently bound to silica, and each individual particle is around 100 nm in size.[16] A model of this molecule and its synthesis can be seen in Figure 3 below. This systems interactions with copper and zinc metal ions were then studied, as well as its interactions with Aβ. While their work found this to be effective at decreasing Aβ aggregation, its synthesis is time-intensive, and they are made in single particles. Additionally, the cyclen is exposed to the environment, and it is

not blocked from intermolecular interactions between other particles. Because metal chelators are not discriminatory in what metals they capture, there are more opportunities for these chelators to capture metal ions that are not directly affecting Aβ before reaching this area of the brain.

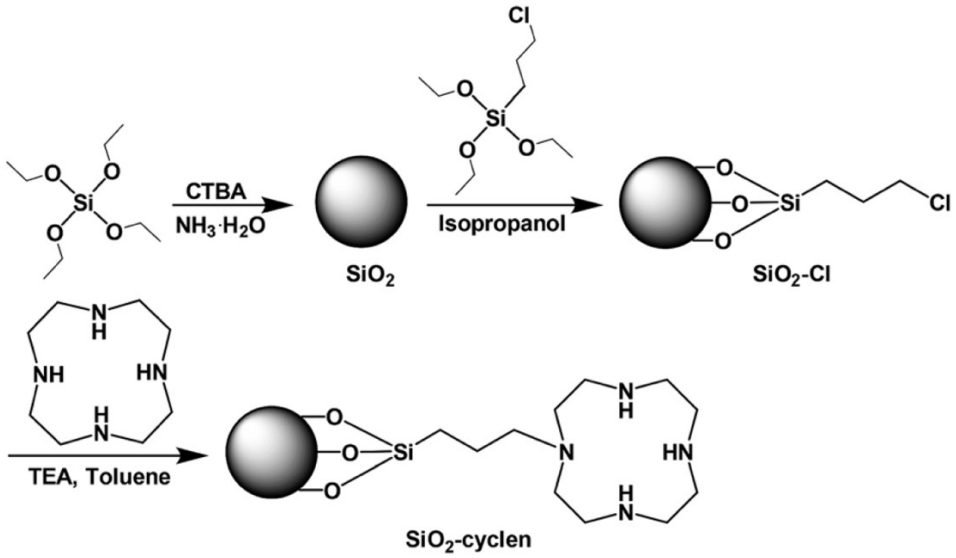

Figure 3. Synthesis route of silica covalently binding to metal chelator.[16]

Using mesoporous silica as a delivery system, a previous student of the Coffer Research Group, Youanna Ibrahim, studied the release of pyclen ligands from mesoporous silica to understand how ligand interactions with $pSiO_2$ effected the release of ligands.[19] A comparison of these two methods can be seen in Figure 4. In both this work and the work of Wang et al., the delivery system is meant to travel across the BBB with the ligand. After crossing the BBB, the ligand would ideally release from the delivery system and perform its function as a metal ion chelator. By loading these ligands into $pSiO_2$, their intermolecular interactions with the environment are limited, and they may have more success in binding the metal ions which are causing damage in the brain.

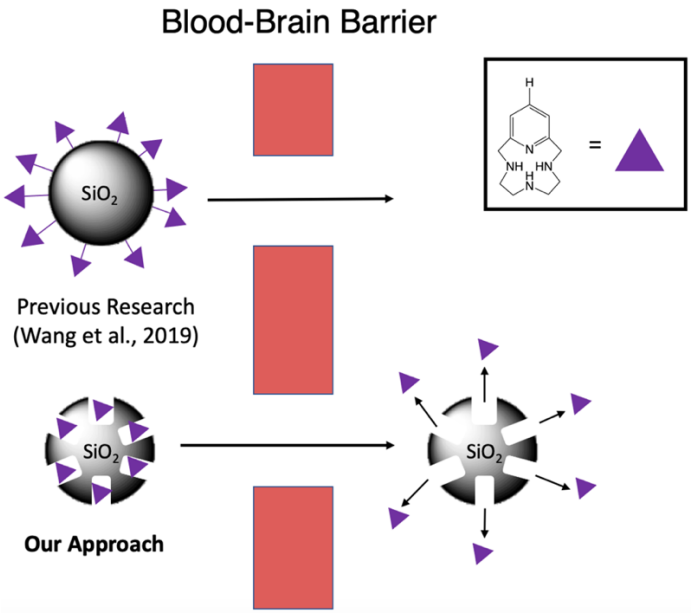

Figure 4. Comparison of delivery system approaches for ligand delivery.

She studied the release of L1, L2, & L3 metal chelators from porous silica in the presence of HEPES buffer alone and HEPES buffer with Cu^{2+} metal ions present.[19] The presence of Cu^{2+} metal ion allowed for the understanding of how these ligands would interact with metals in a solution that mimics a physiological pH and environment.

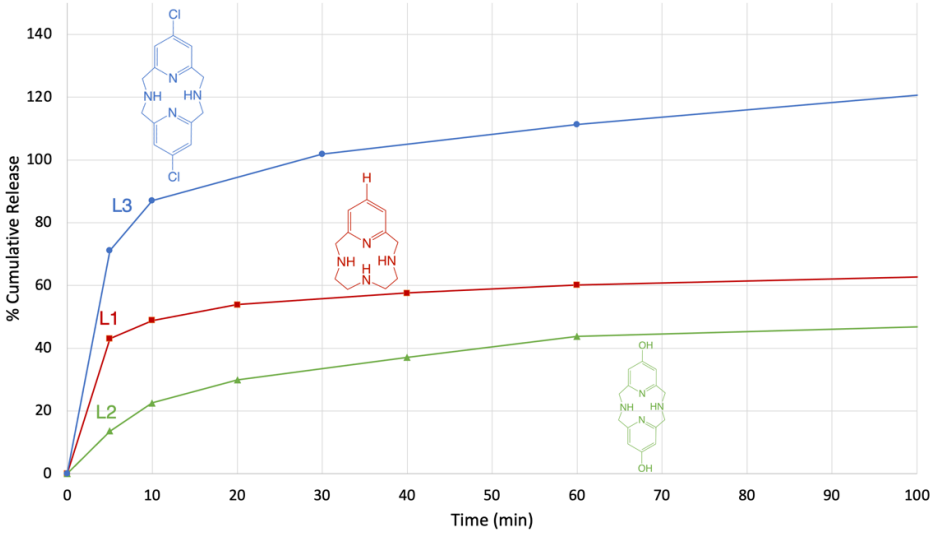

Figure 5. Cumulative Release of L1, L2, & L3 from $pSiO_2$ in HEPES buffer, courtesy of Youanna Ibrahim.[19]

Her results, displayed in Figure 5, show the release of L1-L3 from $pSiO_2$ in HEPES buffer. These results show that while one dimer macrocycle, L3, released at a higher rate, the other dimer, L2, did not. However, this could be due to properties other than size and sterics. There is a possibility that dimer macrocycles L2 and L3 were not as well embedded into the $pSiO_2$ pores as well as other macrocycles simply due to their sizes, which is supported by their lower loading capacities compared to pyridine-monomer pyclen, L1. However, L2 did not experience the same enhanced release as L3. This is possibly a result of hydrogen bonding between hydroxyl functional groups on L2 and the oxygen atoms in $pSiO_2$. Another potential reason for this effect is interactions with surface silanol groups, which could also be interacting with hydroxyl group in L2.

Additionally, data in Figure 6 shows the cumulative release of L1, L2, and L3 from $pSiO_2$ in HEPES buffer in the presence of Cu^{2+} metal ions. This was to observe how metal ion presence impacted release.

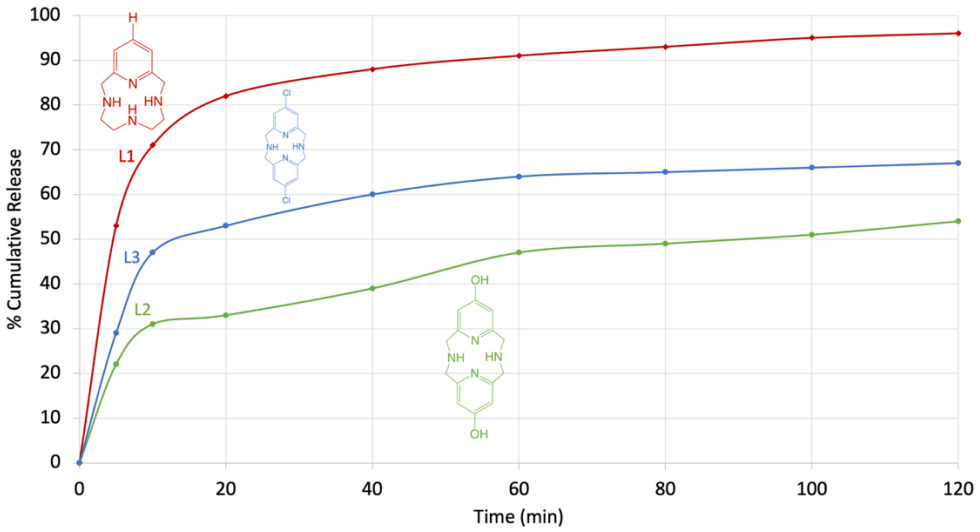

Figure 6. Cumulative release of L1, L2, & L3 from $pSiO_2$ in HEPES buffer in the presence of Cu^{2+} metal ions, courtesy of Youanna Ibrahim.[19]

In the presence of Cu^{2+} metal ions, both dimer macrocycles, L2 and L3, exhibited a lower release profile. The binding constants of L1 through L4 in the presence of Cu^{2+} metal ions are as

follows; 20.644, 21.05, 17.1, and 19.16, respectively.[18] L2 remained releasing less than other macrocycles, and this is likely again due to the presence of hydrogen bonding between hydroxyl groups of the macrocycle and oxygen in porous silica.

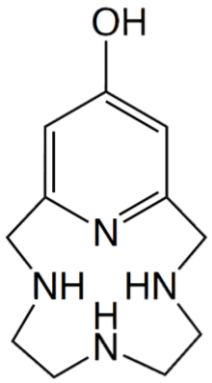

Figure 7. The structure of ^{HO}PyN3 (L4).

To build on Ibrahim's work, this project investigates the release of L4, as seen in Figure 7, from $pSiO_2$ both in the presence of HEPES buffer alone and in the presence of HEPES with Cu^{2+} metal ions. Investigating this macrocycle allows for a better understanding of the roles that the hydroxyl functional group versus the number of pyridine moieties play in determining release rate. Additionally, L2 faced solubility issues in the presence of Cu^{2+} metal ions in HEPES buffer, by studying the pyridine monomer with a hydroxyl group, this solubility issue can hopefully be avoided while still having the highly antioxidant hydroxyl substituted pyridine group present. This work also includes protein aggregation experiments, studying these metal chelators in the presence of Aβ to understand how they impact protein aggregation in the presence of metal ions. In this study, turbidity assays were used to understand protein aggregation. Turbidity assays examine and compare solution cloudiness against a blank to qualitatively examine the turbidity of a solution. Turbidity assays are measured using the same instrumentation as colorimetric assays. However, instead of using a colorimetric reagent or assay to assess protein concentration, a turbidity assay takes advantage of light scattering that occurs when aggregated protein solutions are analyzed.

When light shines on samples containing aggregated protein, light will scatter off of protein aggregates, creating a measurement known as optical density.[12] Increased absorbance values suggest increased amounts of aggregated protein in solution.

2. Experimental Information

2.1 Instruments Used

The following instrumentation were used in this research:

- UV-Vis Spectrophotometer- Aligent Model: Cary 60
- BioTek Synergy H1 Microplate Reader
- VWR Incubating Orbital Shaker
- Thermo Scientific mySPIN 12 Centrifuge
- Buchi Rotary Evaporator
- Mesoporous Silica, Sigma-Aldrich, 1µm particle size, 2nm pore size
- HEPES

Release from Silica Experiments

2.2 Making base form of chelating agents

The base form of chelating agents is more optimal to achieve a slower release profile because at higher pH values, the nitrogen atoms are deprotonated and are better chelating agents to the metal. The chelating agents, courtesy of Dr. Green, are given as HCl salts. To transform these acid salts into a free base form, a given pyclen derivative is dissolved in water, and sodium hydroxide is added to raise the pH of the solution to above 12. Using a Rotary Evaporator, excess water is removed, leaving only the chelating agents. Excess salts are removed using ethanol, and solution is dried overnight in a vacuum-sealed oven.

2.3 Incipient Loading of Pyclen derivatives into porous silica

The incipient loading protocol sought to load pyclen into porous silica to a loading capacity of 25%, by mass. Pyclen derivatives are dissolved in a minimal amount of ethanol. Porous silica is incubated in the orbital shaker at 37° C. In 100 µL increments, pyclen dissolved in ethanol was added to porous silica. After this, the porous silica sat for a period of time to allow ethanol to evaporate. This was repeated until all ethanol with dissolved pyclen had been added to the porous silica, thereby "loading" it. This was then placed in a vacuum overnight to remove excess ethanol.

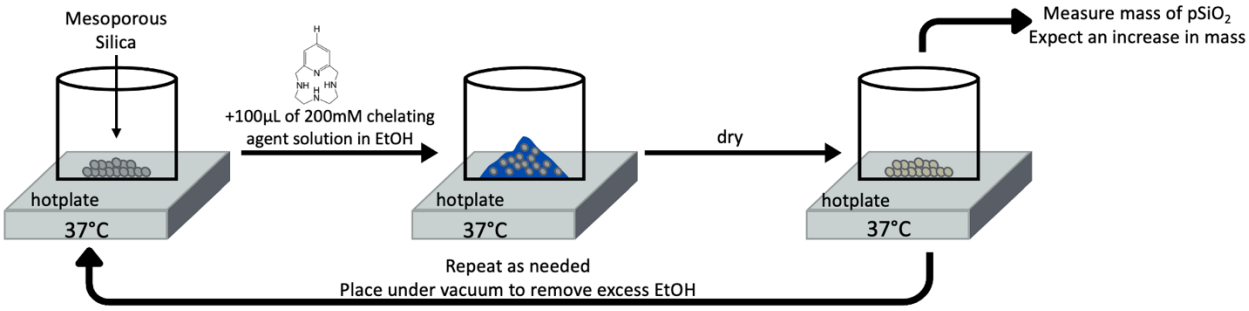

Figure 8. Scheme of Incipient Loading Protocol.

2.4 Loading Capacity

Loading capacity (LC) is used in this research to determine how much pyclen was successfully loaded into porous silica. By design, the mass of pyclen to porous silica should be around 25%. However, understanding that incipient loading is not a perfect protocol, it is understood that some pyclen may not entirely be loaded into the porous silica. Therefore, studying how much was successfully loaded allows for a better understanding of release data for a given loading. An ideal, experimental LC would be close to but not exceeding the theoretical LC, which is calculated using the equation below:

$$\frac{mass\ of\ pyclen}{mass\ of\ pSiO_2} \times 100 = loading\ capacity$$

Loaded $pSiO_2$ was incubated in DMSO to extract out all possible ligands. The DMSO supernatant containing pyclen was measured under UV-Vis Spectroscopy, and the concentration of ligand was determined from a standard curve.

2.5 Release into HEPES buffer

To monitor release, exactly 1mL of HEPES buffer is added with a micropipette to a known mass of loaded porous silica. HEPES buffer is used as the solution buffer due to its similarity to the bodily environment and pH. After incubation for a set amount of time, this solution is centrifuged at 5,000 rpm for two minutes, separating any "released" pyclen from the insoluble porous silica. The supernatant is removed after centrifugation, and its absorbance is measured with UV-Vis spectroscopy. After the supernatant is removed, another aliquot of fresh HEPES buffer is added to the same porous silica and incubation continues. The supernatant is removed for UV-Vis analysis at the following time points: 5, 10, 20, 40, 60, and 120 minutes. This procedure was repeated with HEPES buffer and HEPES buffer that included 4 mM Cu^{2+} metal ions present.

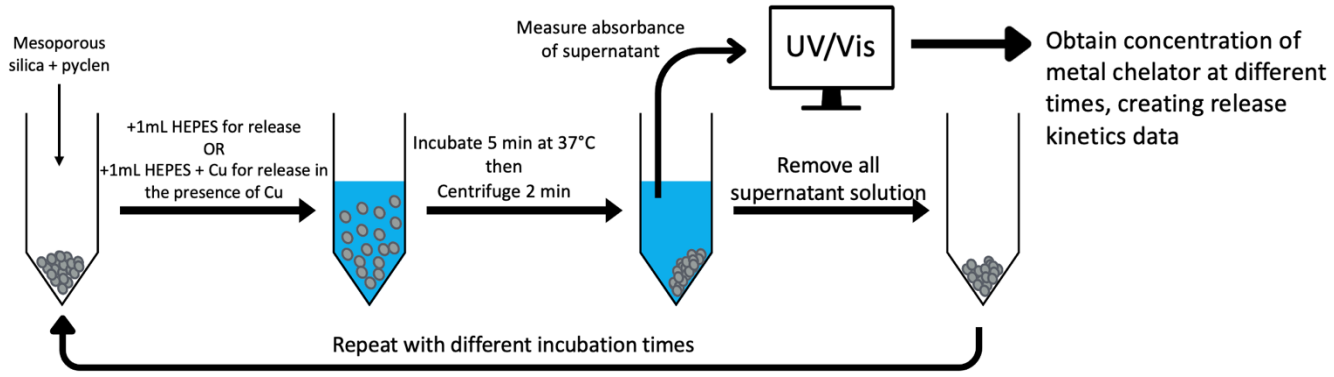

Figure 9. Scheme of Release Experiment Protocol.

Protein Assay Experiments

2.6 Solution Preparation

Solutions of Aβ, Cu^{2+} ions from Copper Sulfate, and ligands L1 through L4 were created separately in HEPES buffer to be incubated together for various assays. For all protein assays

conducted, six experimental groups were utilized for points of comparison. These groups are as follow:

1. Aβ alone [200 μM]
2. Aβ [200 μM] and Cu^{2+} [400 μM]
3. Aβ [200 μM], Cu^{2+} [400 μM], and L1 [800 μM]
4. Aβ [200 μM], Cu^{2+} [400 μM], and L2 [800 μM]
5. Aβ [200 μM], Cu^{2+} [400 μM], and L3 [800 μM]
6. Aβ [200 μM], Cu^{2+} [400 μM], and L4 [800 μM]

Aβ alone was important to study how Aβ would react in HEPES buffer alone, without any interference of Cu^{2+} metal ions or metal chelators, acting as a positive control to understand how much Aβ would remain soluble after an incubation period in the system used. Aβ and Cu^{2+} without any metal chelators present was important for understanding what free metal ions would do to Aβ. This served as the negative control, as it would generate the most aggregated protein and least amount of soluble protein remaining after incubation periods. Experimental Groups 3 through 6 add studied metal chelators to examine how these potentially prevent Aβ aggregation. The amount of protein aggregation in groups 3 through 6 should ideally lie somewhere between the "Aβ alone" and "Aβ and Cu^{2+}" groups, as the presence of metal ions would cause some aggregation, more than any amount occurring in the positive control group, but the presence of the metal chelators would hopefully prevent as much extensive aggregation, creating less aggregation than that in the negative control.

Solutions of each of these experimental groups were created, using 200μM Aβ, 400μM Cu^{2+}, and 800μM metal chelator concentrations. Solutions each had a total volume of 120μL, with equal volume aliquots of each solution being added (40μL each). In experimental groups 1 and 2 where

not all three components were utilized, the volume was brought to 120µL using HEPES buffer. These volumes were based off of Lincoln et al.'s turbidity assay designs.[12]

2.7 *Turbidity Assays*

The order of component addition to Aβ solution created a "preventative" experimental design. After Aβ 40µL aliquots are created, 40µL aliquots of pyclens were added to groups 3 through 6, and these groups are incubated at room temperature for 5 minutes. After this period, 40 µL aliquots of Cu^{2+} metal ions and any necessary HEPES buffer are added to solutions to bring to consistent total volume and these solutions incubate for 24 hours at 37° C in the orbital shaker. After 24 hours, solutions are transferred to a 96-well plate, where 20µL of solution is diluted with 180µL of HEPES in each well.

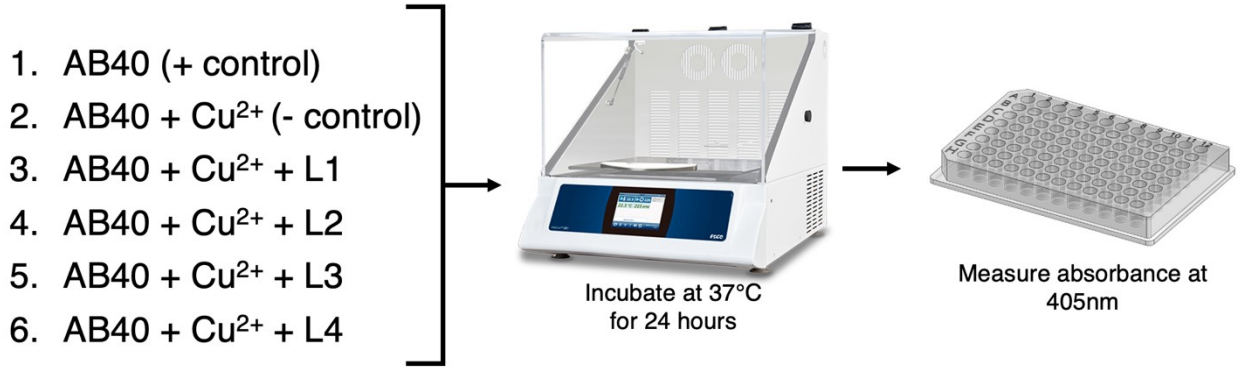

Figure 10. Scheme of Turbidity Assay protocol.

The absorbance of the 96-well plate is taken using the Microplate reader at a wavelength of 405-nm. The blank reading used for these assays was 200µL of HEPES buffer in wells, as this would have no protein to potentially cause any aggregation.

3. Results & Discussion

3.1 Loading Capacity

$^{HO}PyN_3$ (L4) loading capacity was studied using the same procedures as previous ligands to monitor release. Calibration curves in HEPES and DMSO were used to calculate concentration of released pyclen in experimental solutions.

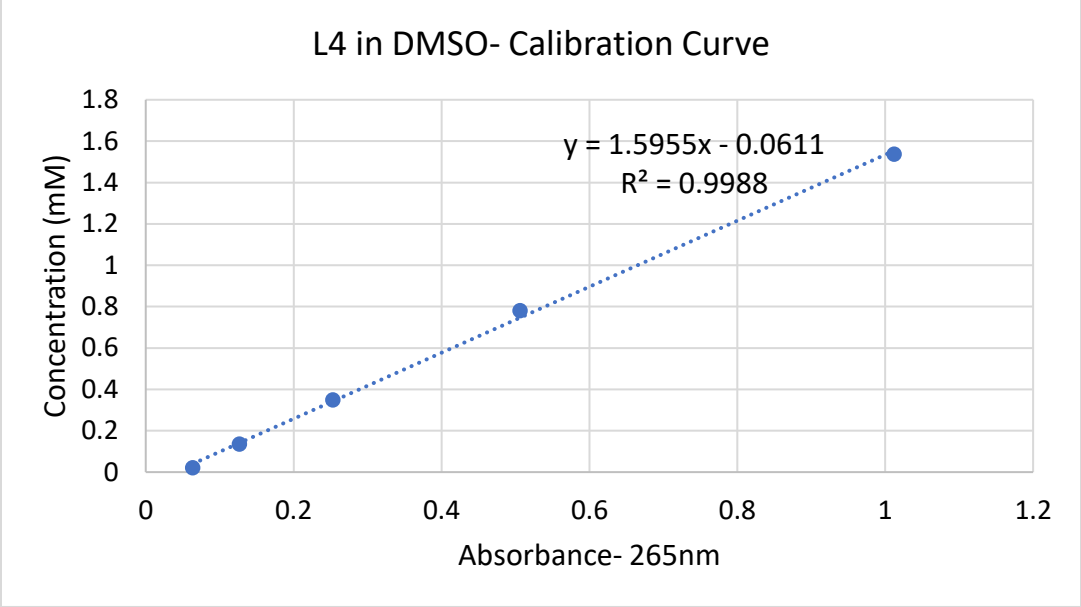

Figure 11. $^{HO}PyN_3$ (L4) in DMSO Calibration Curve.

UV-Vis spectra was analyzed at a wavelength of 265-nm in DMSO solutions. Loading capacity for L4 was measured to be 25.49%. The theoretical loading capacity for this loading was 25.66%. This indicates that 99.3% of HO-PyN3 added was successfully loaded into $pSiO_2$. The loading capacities of all ligands in this study, including L4, are listed below in Figure 12.

Pyclen Molecule	Loading Capacity
L1	17%
L2	10%
L3	16%
L4	25%

Figure 12. Loading Capacity Values for L1-L4.

3.2 $^{HO}PyN_3$(L4) Release Studies

L4 achieved sustained release from HEPES, similarly to other chelators. Its calibration curves in HEPES and HEPES + Cu (II) ions are shown below.

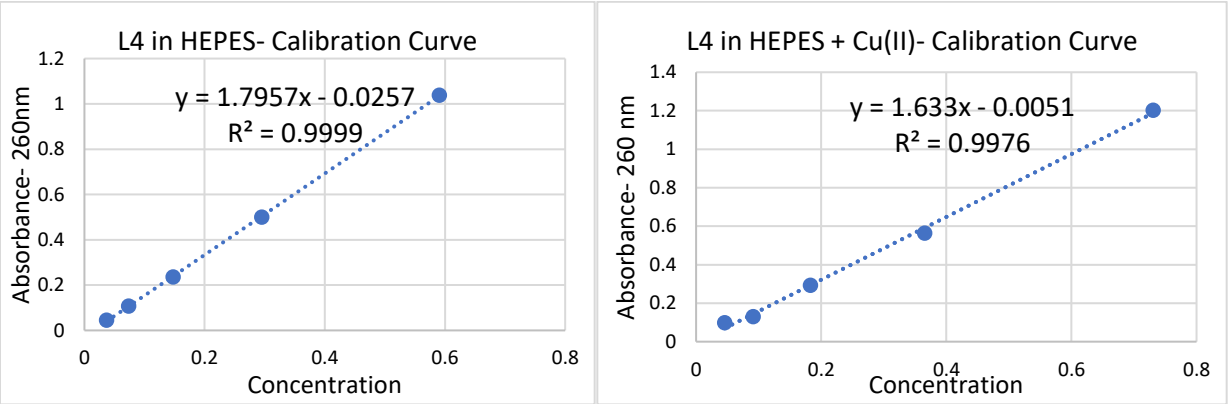

Figure 13. $^{HO}PyN_3$ (L4) Calibration Curve in HEPES buffer and HEPES + Cu^{2+} metal ions

Using known amounts of pyclen in solution allowed for a corresponding absorbance value to be assigned and a coefficient for calculating the concentration of pyclen released from HEPES during release studies. The results of $^{HO}PyN_3$ (L4) release studies are shown individually in Figure 14 and shown in comparison with L1 through L3 in Figure 15.

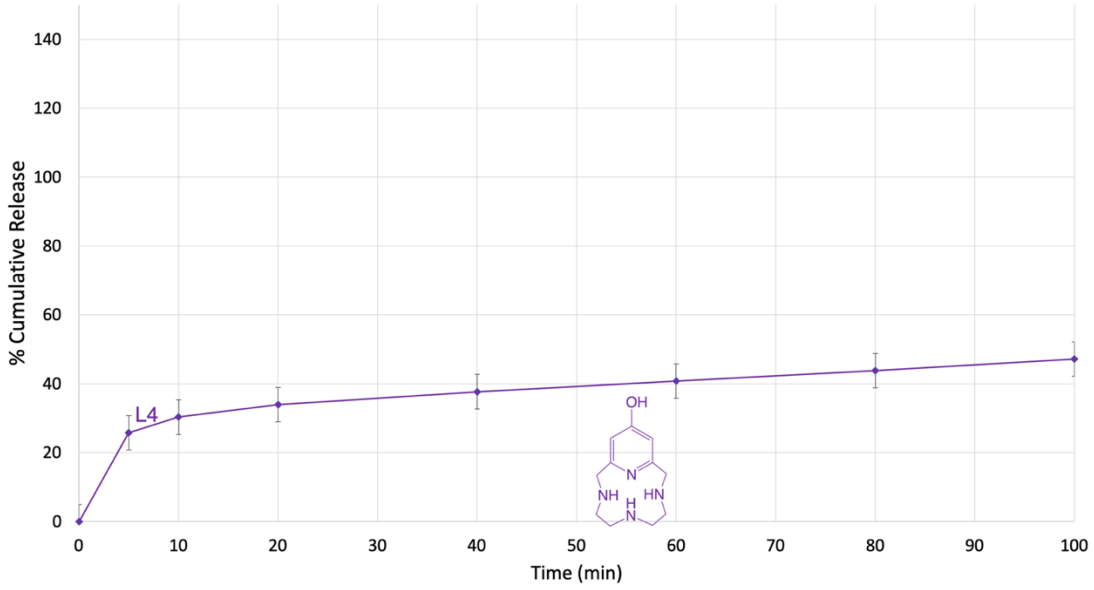

Figure 14. Release of $^{HO}PyN_3$ (L4) from HEPES buffer.

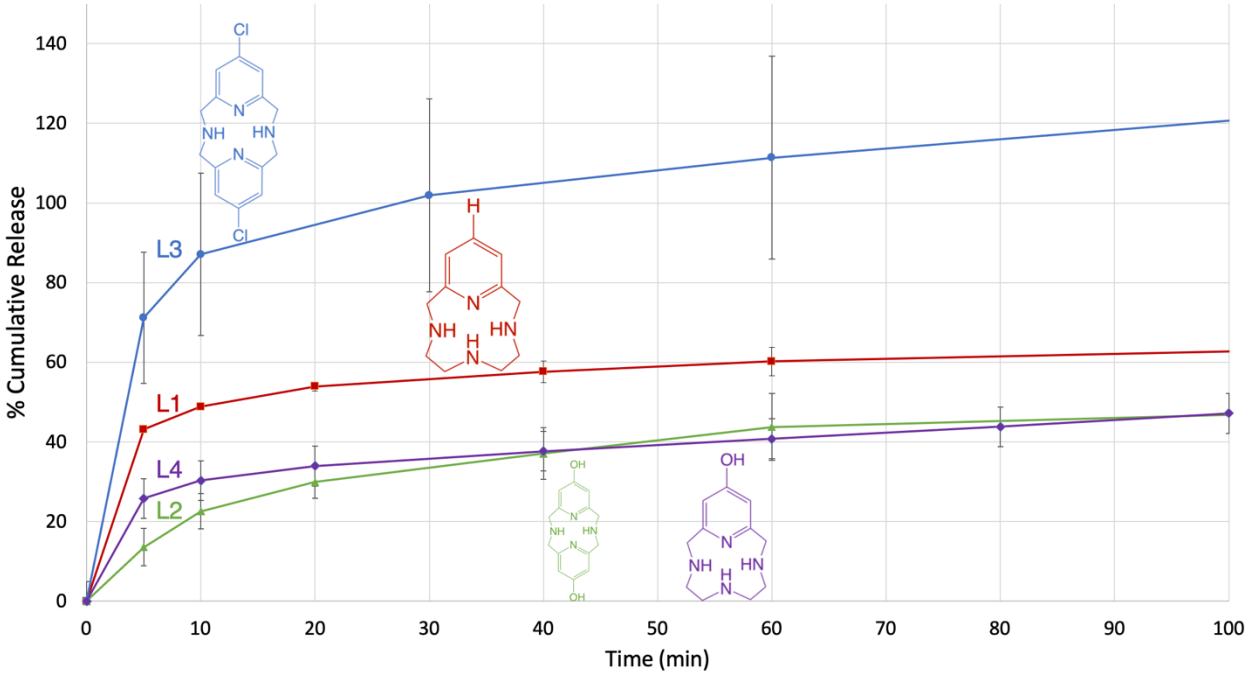

Figure 15. Release of Pyclen Derivatives L1-L4 into HEPES Buffer.

L4 performed similarly to L2, both of which appeared to not release out of $pSiO_2$ as much as L1 and L3 did. This may be the result of hydrogen bonding between the hydroxyl groups of the ligands and the porous silica, which explains the consistent result between both the mono- and di-substituted pyridine ligands. L3 appears above 100%, which is likely additional ethanol contributing to the mass of ligand trapped in the pores. L1, the parent pyclen ligand, has a steady release curve that does not seem to indicate trapping or any strong interactions between the pyclen ligand and the porous silica surface. Despite having a similar cumulative release, L2 appears to have a slower initial release compared to L4, which experiences more of a burst effect. This is likely due to L2's relatively larger size compared to L4, making it more difficult to maneuver out of the pores of mesoporous silica.

3.3 L4 Release from HEPES + Cu^{2+} metal ions

Release experiments identical to those detailed above were carried out in the presence of Cu^{2+} metal ions to understand how the presence of metal ions impacted pyclen release into

solution. The $^{HO}PyN_3$ (L4) release study results are shown individually in Figure 16 and shown in comparison to L1 through L3 in Figure 17.

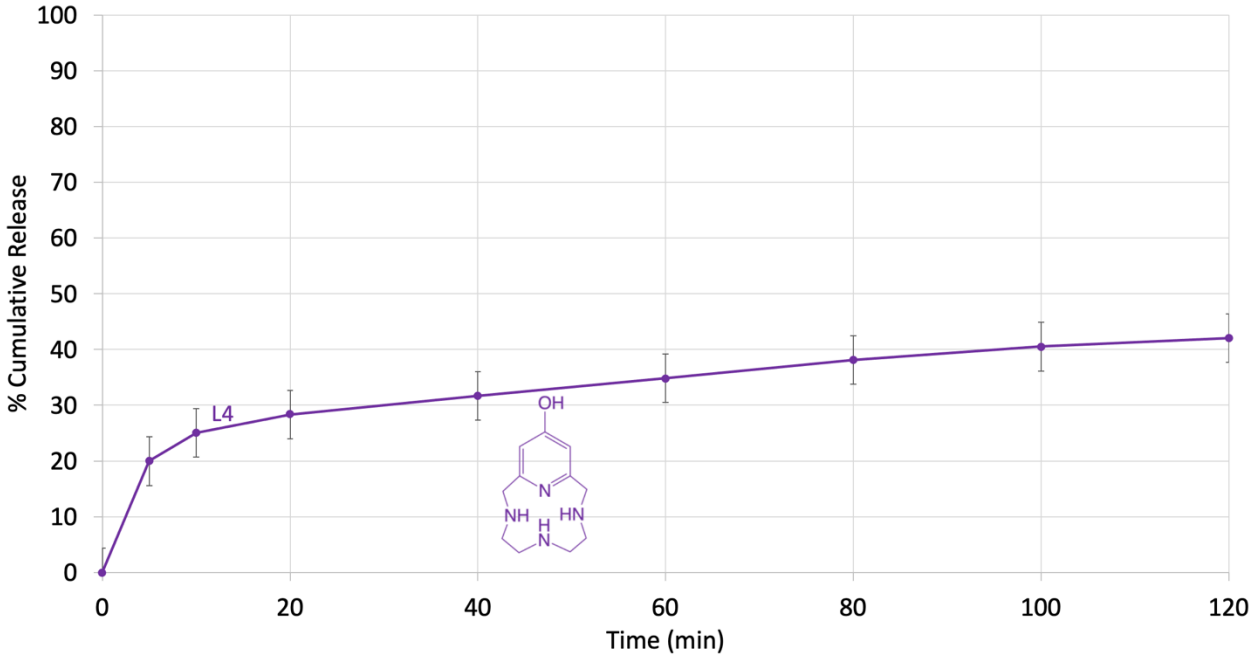

Figure 16. Release of L4 from HEPES + Cu^{2+} metal ions.

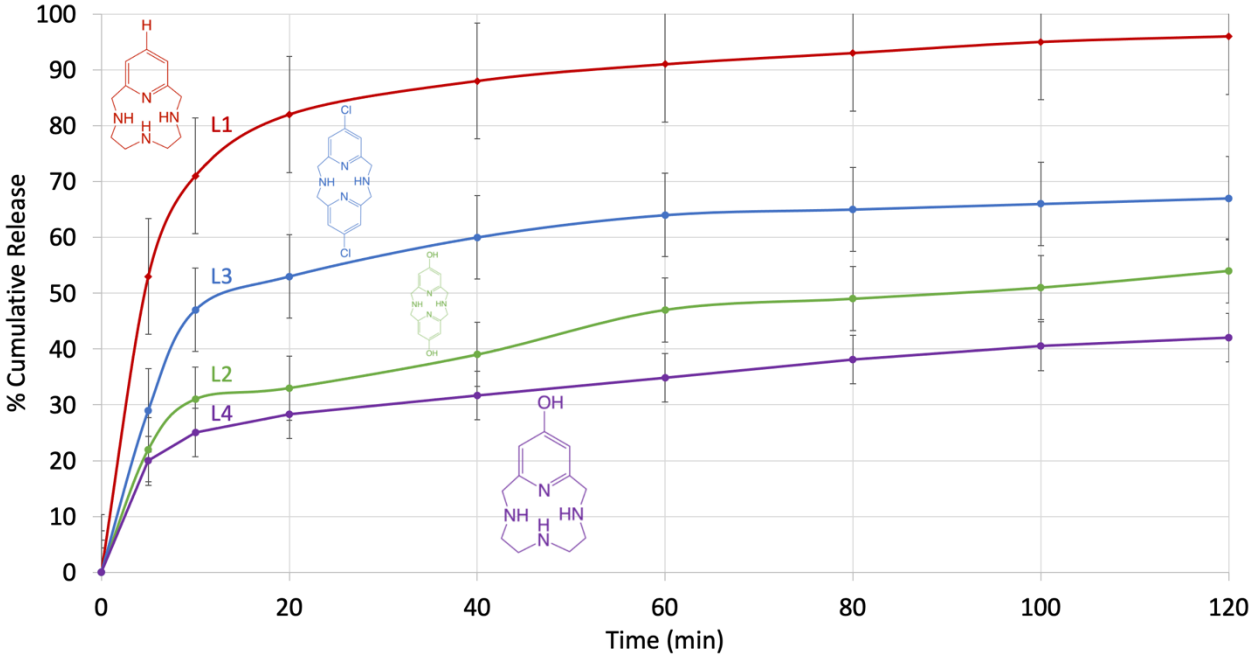

Figure 17. Release of L1-L4 from HEPES + Cu^{2+} metal ions.

All four pyclen derivatives were able to successfully achieve sustained release in the presence of HEPES buffer and Cu^{2+} metal ions. L2 and L4 again exhibit the lowest cumulative amount of released pyclen, likely due to hydrogen bonding with the mesoporous silica surface, creating more interactions that elicit a slower release profile.

3.4 Turbidity Assays and other protein assays

Protein assays that measured amounts of soluble versus aggregated Aβ protein proved difficult to conduct successfully. Initially, experimental designs were modeled from Wang et al., which used a Micro BCA Assay to measure concentrations of remaining soluble protein after incubation with metal ions.[16] However, issues with this assay were quickly discovered when reagent addition to solutions created intense, dark-violet solutions, indicating protein concentrations much higher than possible given the amounts of protein known to be present, as seen in Figure 18.

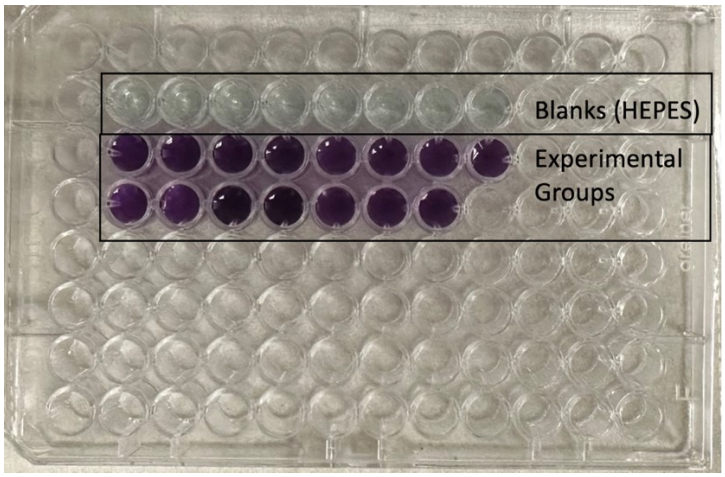

Figure 18. Micro BCA Assay Plate Results.

Upon further investigation of chemical mechanism of a Micro BCA assay, it was discovered that a part of the mechanism of action of this assay is Cu^{2+} metal ion chelation. When Cu^{2+} metal ion is additionally present in solution, as it was in experimental assays, solutions appear much darker, indicating much higher protein concentrations than those present in solution. The

chemical reaction that occurs between the protein solution and working reagent of a Micro BCA assay is shown in Figure 19.

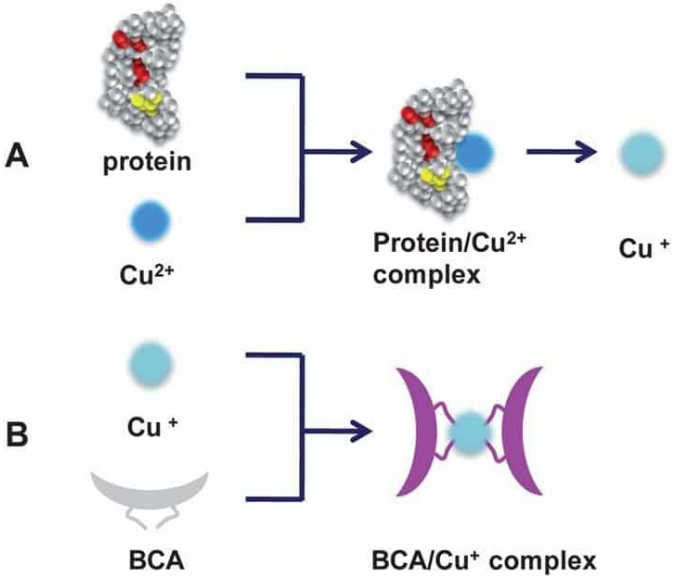

Figure 19. Colorimetric reaction mechanism of Micro BCA Assay.[17]

After Micro BCA Assays proved to be a non-effective way to analyze the solutions of interest, Bradford assays were touted as a possible assay to analyze protein aggregation and concentration.

Turbidity Assays were eventually settled upon as the assay of choice to try to begin understanding the protein behavior in the presence of these ligands and Cu^{2+} metal ions. The turbidity assay conducted utilized a preventative protocol, meaning that pyclen ligands were added to the protein solution before Cu^{2+} metal ions were added. The goal of this was to see if these ligands could prevent the aggregation of Aβ when Cu^{2+} metal ions were then incorporated into the solution. The results of turbidity assays are shown in Figure 20. The results are shown as a percentage of aggregation, with the "AB + Cu" group set to 100% aggregation.

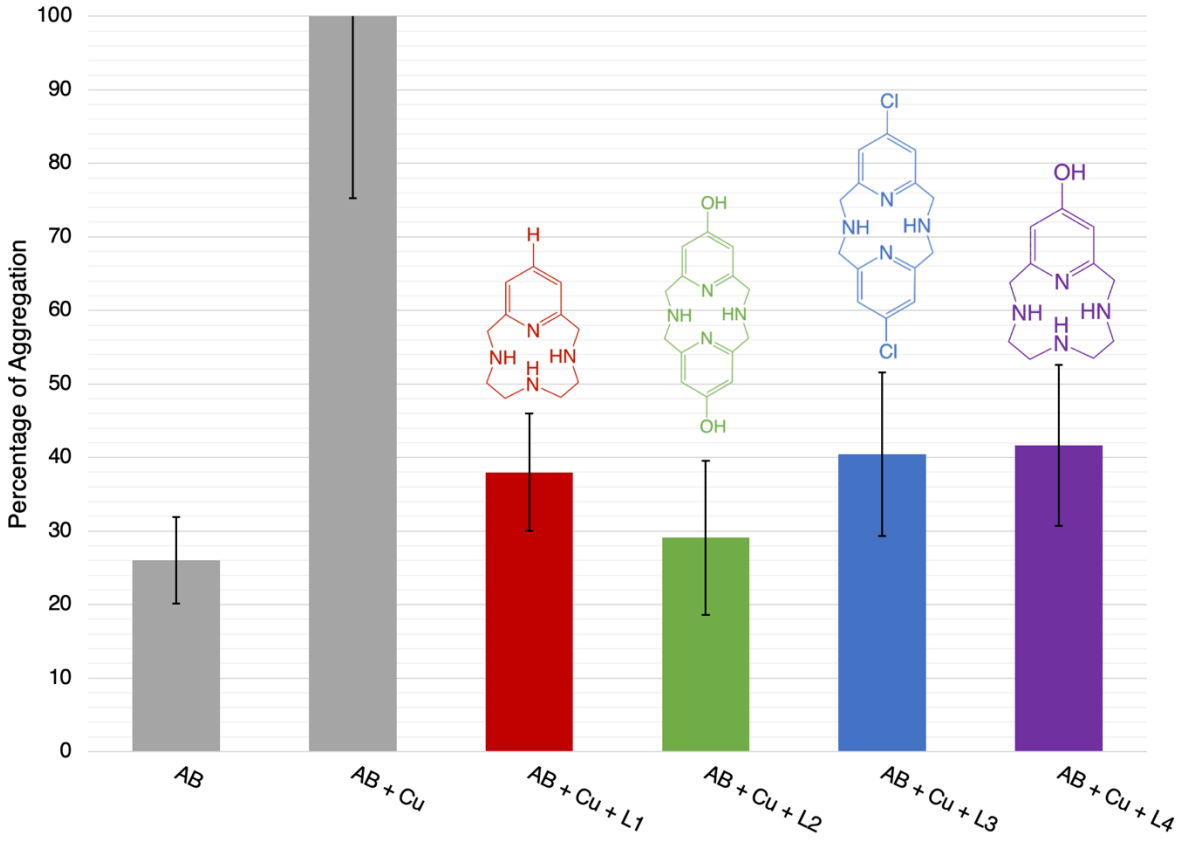

Figure 20. Turbidity Assay Results, represented as percentage.

The turbidity assay results were verified by the results of "AB" and "AB + Cu" experimental groups. "AB + Cu" having the highest levels of absorbance suggest the most protein aggregation occurred in this experimental group. Subsequently, the experimental group "AB" having the lowest level of absorbance is also expected, as this is associated with the least amount of protein aggregation. Experimental groups where metal chelators were present all saw lower levels of aggregation than when only Cu^{2+} metal ions were in solution with Aβ, suggesting that these chelators all successfully prevented protein aggregation in the presence of Cu^{2+} metal ions.

ANOVA						
Source of Variation	*SS*	*df*	*MS*	*F*	*P-value*	*F crit*
Between Groups	0.00031599	5	6.3199E-05	16.4224273	1.7566E-06	2.71088984
Within Groups	7.6967E-05	20	3.8483E-06			
Total	0.00039296	25				

Figure 21. ANOVA Statistical Test Results, Analysis of Turbidity Assay.

Based on the results of ANOVA statistical analysis, as seen in Figure 21, there was statistically significant differences between the means of the groups ($p<0.05$).

4. Conclusion

This work showed the ability of metal chelators L1 through L4 to release from mesoporous silica as a sustained release profile. Additionally, turbidity assays showed these pyclen ligands demonstrated the ability to successfully inhibit protein aggregation through metal chelation.

Many possible directions can be taken to continue this research topic and explore the implications of using mesoporous silica as a delivery system for this pyclen library. Ideas include expanding the pyclen library to include pyclen with various substitutions to understand how these substitutions may impact release and protein aggregation. Additionally, improvements to the release study protocol can be made by creating a more authentic blood-brain barrier model to see how this would impact release. Additional information about protein aggregation can be collected from turbidity assays by incubating protein solutions first with Cu^{2+} metal ions, followed by metal chelators. This approach examines the ability of the chelators to disaggregate proteins after interactions with metal ions.[12] Other directions include using a different protein assay to increase

our understanding of protein aggregation behavior in the presence of metal ions and our chosen pyclen library. A western blot is a potential protein assay that could be used in the future for this purpose. Future protein assays can hopefully incorporate porous silica into them as another variable to study how silica would interact with and potentially impact Aβ.

This work goes to show the advantages of mesoporous silica as a delivery system of these therapeutics because of its biocompatibility, tunability, and ability to achieve a diffusion-limited sustained release profile. Turbidity assays also showed the ability of these ligands to bind Cu^{2+} metal ions and prevent Aβ aggregation.

References

1. Alzheimer's Association Website, *2024 Alzheimer's Disease Facts and Figures*. Alzheimer's Association, 2024. https://www.alz.org/alzheimers-dementia/facts-figures (accessed 2-24-24).

2. *Mayo Clinic Alzheimer's Disease Information Page*. https://www.mayoclinic.org/diseases-conditions/alzheimers-disease/symptoms-causes/syc-20350447 (accessed 2-24-24).

3. Hardy, J. A.; Higgins, G. A. Alzheimer's disease: the amyloid cascade hypothesis, *Science*. **1992**, *256*(5054), 184-185. DOI: 1126/science.1566067

4. Hardy, J.; Selkoe, D. J. The amyloid hypothesis of Alzheimer's disease: progress and problems on the road to therapeutics. *Science* **2002**, *297*(5580), 353– 356. DOI: 10.1126/science.1072994

5. Penke, B.; Szűcs, M.; Bogár, F. Oligomerization and Conformation Change Turn Monomeric β-Amyloid and Tau Proteins Toxic: Their Role in Alzheimer's Pathogenesis. *Molecules*, **2020**, *25*(7), 1659. https://doi.org/10.3390/molecules25071659

6. Kreiser, R. P.; Wright, A. K.; Block, N. R.; Hollows, J. E.; Nguyen, L. T.; LeForte, K.; Mannini, B.; Vendruscolo, M.; Limbocker, R. Therapeutic Strategies to Reduce the Toxicity of Misfolded Protein Oligomers. *Int J Mol Sci*, **2020**, *21*(22), 8651. https://doi.org/10.3390/ijms21228651

7. Chia, S.; Cataldi, R. L.; Ruggeri, F. S.; Limbocker, R.; Condado-Morales, I.; Pisani, K.; Possenti, A.; Linse, S.; Knowles, T. P. J.; Habchi, J.; Mannini, B.; Vendruscolo, M. A Relationship between the Structures and Neurotoxic Effects of Aβ Oligomers Stabilized by Different Metal Ions. *ACS Chem Neurosci,* **2024**, *15*(6), 1125-1134. https://doi.org/10.1021/acschemneuro.3c00718

8. Liu, F.; Zhang, Z.; Zhang, L.; Meng, R.; Gao, J.; Jin, M.; Li, M.; Wang, X.; Effect of metal ions on Alzheimer's disease, *Brain and Behavior* **2021,** *12*(3), 1-9. DOI: 10.1002/brb3.2527.

9. Kitazawa, M.; Cheng, D.; LaFerla, F. M.; Chronic copper exposure exacerbates both amyloid and tau pathology and selectively dysregulates cdk5 in a mouse model of AD, *Journal of Neurochemistry* **2009**, *108*, 1550-1560. DOI: 10.1111/j.1471-4159.2009.05901.x

10. Chaudhari, V.; Bagwe-Parab, S.; Buttar, H. S.; Gupta, S.; Vora, A.; Kaur, G.; Challenges and Opportunities of Metal Chelation Therapy in Trace Metals Overload-Induced Alzheimer's Disease. *Neurotoxicity Research* **2023,** *41*, 270-287. DOI: 10.1007/s12640-023-00634-7

11. Ling, Y.; Hao, Z.; Liang, D.; Zhang, C.; Liu, Y.; Wang, Y. The Expanding Role of Pyridine and Dihydropyridine Scaffolds in Drug Design. *Drug Des Devel Ther* **2021**, *15*, 4289-4338. DOI: 10.2147/DDDT.S329547

12. Lincoln, K. M.; Richardson, T. E.; Rutter, L.; Gonzalez, P.; Simpkins, J. W.; Green, K. N. An N-Heterocyclic Amine Chelate Capable of Antioxidant Capacity and Amyloid Disaggregation. *ACS Chem Neuro* **2012**, *3*, 919-927. dx.doi.org/10.1021/cn300060v

13. Zha, S.; Liu, H.; Li, H.; Li, H.; Wong, K.; All, A. H. Functionalized Nanomaterials Capable of Crossing the Blood-Brain Barrier. *ACS Nano* **2024**, *18*(3), 1820-1845. https://doi.org/10.1021/acsnano.3c10674.

14. Singh, P.; Srivastava, S.; Singh, S. K. Nanosilica: Recent Progress in Synthesis, Functionalization, Biocompatibility, and Biomedical Applications. *ACS Biomater. Sci. Eng.* **2019**, *5*(10), 4882-4898. https://doi.org/10.1021/acsbiomaterials.9b00464.

15. Argyo, C.; Weiss, V.; Bräuchle, C.; Bein, T. Multifunctional Mesoporous Silica Nanoparticles as a Universal Platform for Drug Delivery. *Chem Mater* **2014**, *26*(1), 435-451. https://doi.org/10.1021/cm402592t

16. Wang, J.; Wang, K.; Zhu, Z.; He, Y.; Zhang, C.; Guo, Z.; Wang, X. Inhibition of Metal-Induced Amyloid β-Peptide Aggregation by a Blood–Brain Barrier Permeable Silica–Cyclen Nanochelator. RSC Advances 2019, 9 (25), 14126–14131. DOI: 10.1039/c9ra02358e

17. *BCA Colorimetric Protein Assay.* https://onelab.andrewalliance.com/library/bca-colorimetric-protein-assay-X5nPg0gP (accessed 4-1-2024).

18. Smith, K. J.; Schwartz, T. M.; Mekhail, M. A.; Freire, D. M.; Bowers, C.; Nguyen, N.; Green, K. N. Rings of Power: Controlling the SOD Mimic Activity by the Addition of Pyridine Rings within the Pyridinophane Scaffold [Manuscript in Preparation]. **2024**. Texas Christian University.

19. Ibrahim, Y. Enhancing Metal Ion Scavenging Delivery Using Porous Materials. Undergraduate Honors Thesis, Texas Christian University, Fort Worth, Texas, 2022.